

# The fourth UltraVISTA data release

A. Moneti, H. J. McCracken, P. Hudelot, S. Rouberol, O. Herent, Y. Mellier  
(Institut d’Astrophysique de Paris);  
J. Dunlop, O. Le Fèvre, M. Franx, J. Fynbo,  
R. Bowler, K. Caputi, O. Kauffmann, B. Milvang-Jensen (UltraVISTA);  
C. Gonzalez-Fernandez, E. Gonzalez-Solares, M. Irwin, J. Lewis (CASU);  
R. Blake, N. Cross, M. Read, E. Sutorius (WFAU).

March 13, 2019

**Data Collection:** UltraVISTA  
**Release number** 4  
**Data provider:** Jim Dunlop  
**Date:** March 13, 2019

## 1 Abstract

UltraVISTA is an ultra-deep near-infrared survey of the central region of the COSMOS field (Scoville et al. 2007). This document describes the fourth UltraVISTA data release, “DR4” which comprises stacked images and catalogues in  $YJHK_s$  and NB118 narrow-band filter.

### 1.1 Acknowledging these data products

Any publications using these data products must include this text:

“Based on data products from observations made with ESO Telescopes at the La Silla Paranal Observatory under ESO programme ID 179.A-2005 and on data products produced by CALET and the Cambridge Astronomy Survey Unit on behalf of the UltraVISTA consortium.” In addition a reference to the UltraVISTA DR1 survey paper should be included: McCracken et al. (2012).

## 2 Overview of observations

DR4 was built from the pre-processed UltraVISTA images from CASU (“The Cambridge Astronomy Survey Unit”<sup>1</sup>) observed at VISTA from 4 December, 2009 to 29 June, 2016 as available in early 2017. We downloaded 63,931 individual images. After quality control (which mainly is a rejection of images with FWHM  $> 1.0''$  or ellipticity  $> 0.1$ , see Sect. 4.1), we were left with 58,138 individual images that were used to create the 5 stacks for the 5 bands:  $Y$ ,  $J$ ,  $H$ ,  $K_s$ , and NB118. The observation dates of all the individual images used can be found by inspecting the file names of the individual images which are recorded in the provenance tables

---

<sup>1</sup><http://casu.ast.cam.ac.uk>

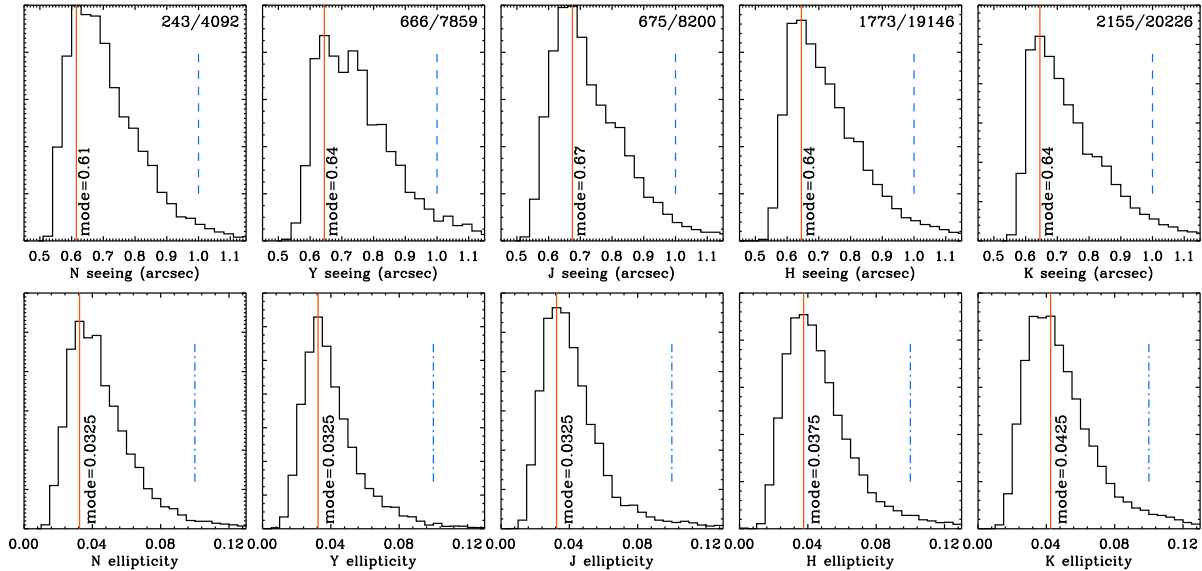


**Figure 1:** FWHM (top) and ellipticity (bottom) distributions for all DR4 images. The red solid line indicates the mode of each distribution, and the blue dashed line shows the cut-off thresholds adopted.

stored in an extension in each image, described in Section 5.1. The total number of observing blocks contributing to the stacks in this release is 1716; the IDs of these OBs are recorded in the headers (keywords `OBID1`, `OBID2`, ...). The total exposure time in this release is 1287.5 hours (cf. keyword `TEXPTIME` in each stack).

This release comprises seven complete observing seasons: however, less data were taken in season 2 (2010–2011) due to the VISTA primary mirror being re-coated during the UltraVISTA observing season. Figure 1 shows the seeing and ellipticity distributions (measured using `PSFex`) on all images which were processed for DR4, separated by filter. The red solid line represents the mode of each distribution, and the blue dashed line shows the cut-off thresholds adopted. In general, the median values in each filter are very similar as a consequence of queue scheduling.

## 3 Release Content

### 3.1 Overview

In this release we provide five stacked images and their corresponding weight maps for  $YJHK_s$  and NB118 narrow-band data taken during the first seven years of UltraVISTA survey operations. In addition, single band individual source lists and source lists created in dual-image mode (using the  $K_s$  image as a detection image) are provided (note that in ESO terminology, single-band tabular data are referred to as “Source lists” and multi-band merged data are referred to as catalogues). We also provide a five-band catalogue that meets the requirement for a catalogue in the Phase 3 framework. The data volume is  $\sim 90$  GB as in DR3. The total survey area is close to  $1.9 \text{ deg}^2$ . Note that, unlike in previous releases, chip 16 has not been masked.

## 3.2 Special image header contents

The files released follow ESO’s Phase 3 standard for the FITS headers, including the type and form of the provided metadata. As previously, we have made a small extension to this scheme in the form of COMMENT FITS header lines to provide additional information related to the particular structure of UltraVISTA. The UltraVISTA field of  $1.5 \text{ deg} \times 1.2 \text{ deg}$  (a VIRCAM tile) does not have a uniform depth; rather the field is covered by 4 *ultra-deep stripes* and 4 *deep stripes*. This is shown in Fig. 1 in McCracken et al. (2012), and it is quantified in the weight maps for each of the 5 stacks that are included in this release.

Specifically, we have set the EXPTIME keyword (giving the typical exposure time per pixel in seconds), to the value for the ultra-deep stripes. And in COMMENT lines we list the value for both sets of stripes, e.g. for the  $K_s$ -band stack:

```
COMMENT ultra-deep stripes: typ. exptime per px = 566580.1 s (keyword EXPTIME)
COMMENT      deep stripes: typ. exptime per px = 304520.0 s
```

Similarly we have set the ABMAGLIM keyword (giving the limiting magnitude) to the value for the ultra-deep stripes, and given the value for both sets of stripes in COMMENT lines, e.g. for the  $K_s$ -band stack:

```
COMMENT ultra-deep stripes: typical ABMAGLIM = 24.9 (keyword ABMAGLIM)
COMMENT      deep stripes: typical ABMAGLIM = 24.5
```

Finally, we follow the standard and provide keywords DIT and NDIT keywords only in the stacks where all the individual images had the same value of DIT and/or NDIT. In all stacks we in COMMENT lines give the breakdown of number of individual images on the different DIT,NDIT combinations, e.g. for the  $K_s$ -band stack:

```
COMMENT Breakdown of the used images on different NDIT,DIT combinations
COMMENT N_images NDIT  DIT
COMMENT      21775    6   10
COMMENT      25      6    1
```

## 4 Release notes

### 4.1 Data reduction and calibration

Previous UltraVISTA releases were processed at the TERAPIX data centre. However, since the founding of TERAPIX in 1997 the data processing needs of the astronomical community have evolved considerably and it was decided to end TERAPIX operations in 2017. TERAPIX has been replaced by a smaller structure CALET<sup>2</sup> (Collaboration for wide-field Astronomy Linked to Euclid and other Telescopes) and an associated processing centre CANDIDE (Computer for Deep Imaging Data for Euclid). As the name suggests, this data centre is primarily dedicated to processing associated ground- and space-based data for Euclid and the Euclid calibration

---

<sup>2</sup><https://calet.org/calet/>

fields including UltraVISTA/COSMOS. This new structure ensures that we have support for processing operations well after the completion of UltraVISTA. During the 2017 transition phase, we adapted the TERAPIX pipeline to run on CANDIDE and validated carefully results from processing on our new hardware.

In early 2017 we downloaded from CASU<sup>3</sup> all available individual sky-subtracted images covering observing seasons 1–7 (namely ca. 64,000 files covering the period from December 2009 to June 2016 (all processed by version 1.3 of the CASU pipeline<sup>4</sup>), the corresponding sky frames (typically one sky frame for each CASU stack of 30 images), flat-fields, bad pixel maps and stacked `_st` images. We reprocessed the full dataset so as to take advantage of various improvements in our processing pipeline.

For DR1 all images were visually inspected but the large number of images in subsequent releases made such manual inspection impractical. Moreover, the majority of the rejected images in DR1 were due to doubled PSFs caused by loss of guiding, a problem which has been subsequently been corrected. These rejected images were also removed from DR4. Following previous releases this was followed by a qualification step that determined the PSF size and ellipticity of each image using `PSFex`: all images with FWHM  $> 1.0$  arcsec or ellipticity  $e > 0.1$ , were rejected. Histograms of these parameters and the thresholds are shown in Figure 1. This selection discarded  $\sim 8.6\%$  of the images, mostly independent of filter band. One important consequence is that the FWHM and ellipticity distributions are nearly independent of filter, making PSF homogenisation for multi-band NIR catalogues only largely unnecessary.

The remainder of the processing followed the method outlined in DR1 (McCracken et al. 2012) and in previous survey release documents. To summarise: we first generate source lists and weight maps from the initial CASU sky-subtracted data, use the source lists to calibrate the astrometry (this time with respect to the Gaia DR1 catalogue) and to perform a relative photometric calibration, and then stack all the images into what we call the *first-pass* stacks. These stacks are used to generate *global* object masks, one per filter, that include faint objects lost in the noise in the individual images. These masks are in turn used to build object masks for the individual images for use in determining the proper sky to subtract.

Prior to determining the sky for each image, the originally subtracted CASU sky is added back in. Then, for each “source” image a sky frame is built from a minimum of 5 and up to 20 other images obtained within 20 min of the “source” image which are masked with the source mask described above, and median (stack) filtered to produce a source-free image, which is subtracted from the “source” image. For a few tens of images (all bands combined) there is not the minimum of 5 nearby images to build a sky frame, and they were rejected.

Finally, destriping (in both  $x$ - and  $y$ - directions) is carried out and large-scale gradients are removed before re-sampling and re-stacking the images onto the COSMOS astrometric grid using a pre-defined tangent point to produce the final stacks and their respective weight maps. Unlike in previous releases (given the much higher precision of the astrometric solution based on the Gaia DR1 catalogue), there is no need to build a new astrometric solution for the sky-subtracted images.

The coadding technique used here is identical to the one used in DR3 and is described in the

---

<sup>3</sup><http://casu.ast.cam.ac.uk/vistasp/>

<sup>4</sup><http://casu.ast.cam.ac.uk/surveys-projects/vista/data-processing/version-log>

DR3 release document<sup>5</sup>. Images and weight maps are coadded using **SWarp** with the “clipped mean stacking” outlier removal technique described in Gruen et al. (2014) with parameters `CLIP_SIGMA=4.0` and `COMBINE_TYPE=CLIPPED`.

## 4.2 Changing the UltraVISTA astrometric reference frame

At the start of COSMOS we used an astrometric catalogue derived from Megacam  $i^*$  band images taken over the full COSMOS field. These images were in turn registered to an external astrometric reference frame. Since then, 2MASS (Skrutskie et al. 2006) has become available and the limitations of the earlier catalogue have become apparent (for example, there is an offset in declination visible in the lower panel in Figure 7 of McCracken et al. (2012)). For DR3 we switched to a reference based on Pan-STARRS Medium-Deep Survey data. With the arrival of the Gaia DR1 (Gaia Collaboration et al. 2016), it was imperative to switch to this new reference (Gaia-DR2 will be used in a future release when **Scamp** will be upgraded to use the proper motions). About 550 Gaia sources are found in the UltraVISTA region.

Thanks to the greater astrometric precision of the Gaia catalogues our astrometry is now tied primarily to this external reference and overlapping sources are correspondingly less important. This has an important consequence of reducing systematic offsets induced by varying numbers of overlapping sources between the deep and ultra-deep regions. This can be seen in Figure 2 which shows the 2D internal and external astrometric accuracy plots produced by **Scamp** for 7254 Y-band images obtained with 2MASS, Pan-STARRS and Gaia (from left to right). The dashed box of 0.344 arcsec on the side represents a pixel. The figures show dramatically how the internal and external astrometric accuracy is improved by switching to the highly accurate and dense Gaia catalogue (note that the scales on these plots from left to right is not the same). For example, for the 20,000 images in the  $K_s$ , internal astrometric precision is now  $\sim 40$  milli-arcseconds (mas) internally and  $\sim 30$  mas externally. Comparing our previous stacks with new Gaia catalogues shows that previous releases may have suffered from systematic errors at the level of 0.1 arcsec (see below).

Finally, one important consequence of switching from 2MASS to Gaia is **that in DR4 there is now an offset in the astrometric co-ordinates of UltraVISTA field compared to previous releases**. This has the immediate practical consequence that for best results in multi-band matched aperture photometry any images in other filters must be shifted to the new Gaia astrometric reference and existing COSMOS images using the old 2MASS astrometric reference should not be used.

## 4.3 Data quality

### 4.3.1 Comparison with 2MASS

In Figure 3 we compare the `mag_auto` magnitudes and the positions of stars in our source list with those in the 2MASS all-sky point source catalogue (Skrutskie et al. 2006). (Note also that 2MASS is used for the initial photometric calibration of the survey by CASU). Of course, a significant limitation of this comparison is that the magnitude range over which sources in UltraVISTA and 2MASS overlap is small, and furthermore that the UltraVISTA instrumental

---

<sup>5</sup>[http://www.eso.org/sci/observing/phase3/data\\_releases/uvista\\_dr3.pdf](http://www.eso.org/sci/observing/phase3/data_releases/uvista_dr3.pdf)

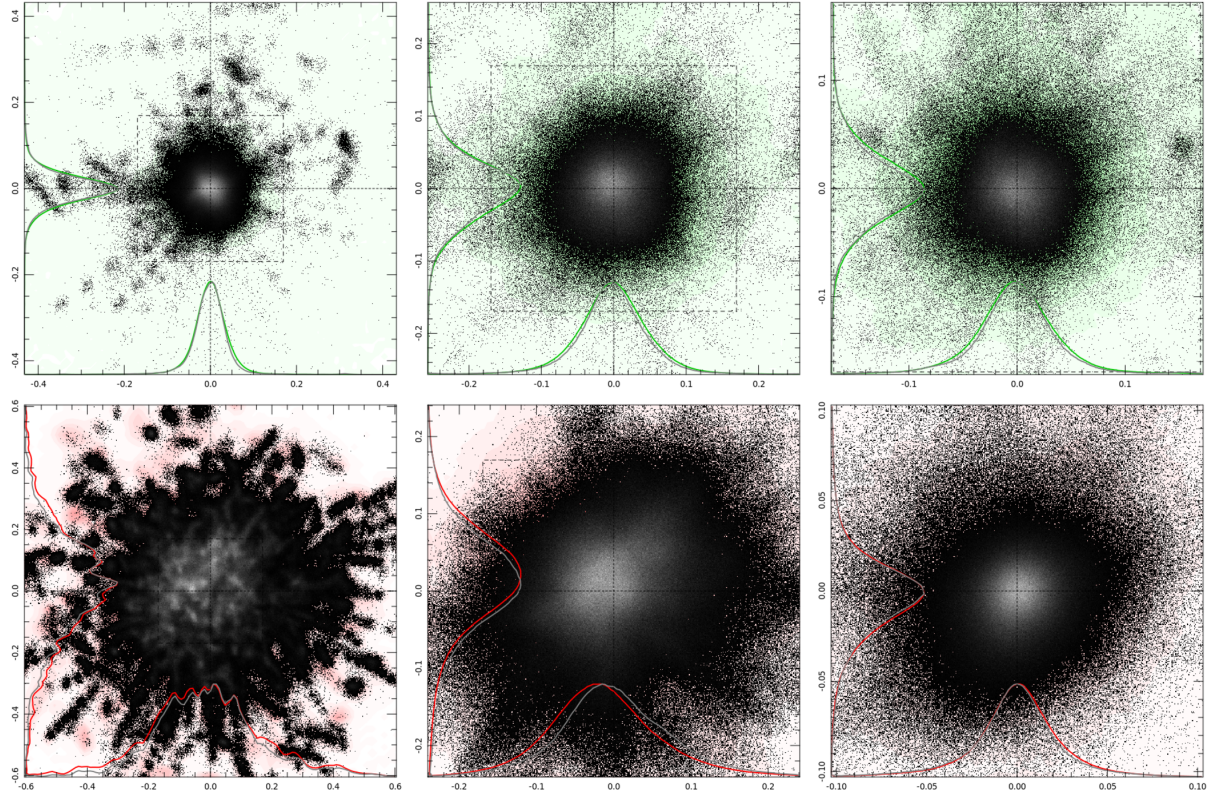


**Figure 2:** Astrometric accuracy from *Scamp*: from left to right are 2MASS, Pan-STARRS, and GAIA-DR1, top is internal, and bottom is external. The scale is in arcsec and the square, dashed box indicates the pixel size (0.344 arcsec). See text for more details.

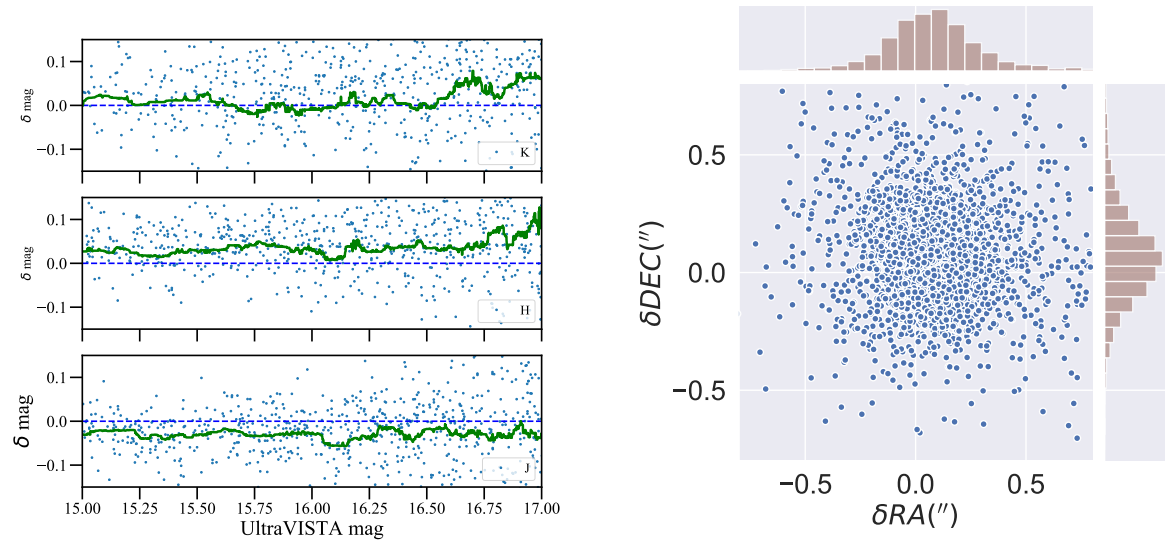


**Figure 3: Comparisons with 2MASS.** Left panel: Magnitude difference  $\delta$  between total  $J$ ,  $H$ , and  $K_s$  magnitudes of stars in UltraVISTA DR4 with sources in 2MASS. The green line corresponds to a running median computed over 100 points. Right panel: Difference in position, in arcseconds, with respect to stars in the 2MASS, as a function of right ascension and declination.

| Filter               | Exposure time<br>per px [hrs] |      | Limiting mag.<br>$5\sigma, 2''$ [AB mag] |      | FWHM<br>[arcsec] | Ellipticity  |
|----------------------|-------------------------------|------|--|------|------------------|--------------|
|                      | Ultra-deep                    | Deep | Ultra-deep                               | Deep | Entire image     | Entire image |
| <i>Y</i>             | 150.2                         | 11.0 | 25.8                                     | 24.7 | 0.77             | 0.01         |
| <i>J</i>             | 154.7                         | 12.8 | 25.6                                     | 24.5 | 0.77             | 0.01         |
| <i>H</i>             | 181.8                         | 13.2 | 25.2                                     | 24.1 | 0.76             | 0.02         |
| <i>K<sub>s</sub></i> | 157.4                         | 84.6 | 24.9                                     | 24.5 | 0.78             | 0.01         |
| NB118                | 92.6                          | 0.0  | 24.4                                     | N/A  | 0.74             | 0.01         |

**Table 1:** Characteristics of the images: typical exposure time per pixel and limiting magnitudes in both deep and ultra-deep regions and PSF FWHM and ellipticity measured in the entire image. **Important note:** The limiting magnitudes listed in this table and in the headers are computed using “empty aperture” measurements in  $2.0''$  diameter apertures, and are subsequently corrected to total magnitude by subtracting 0.3 mag. This is the same procedure used for DR3.

photometric system is not the same as the 2MASS system (this is described in more detail in McCracken et al. 2012). Nevertheless, the result of this test is shown in the left panel of Fig. 3 where we plot UltraVISTA–2MASS magnitudes for all non-saturated stellar sources and with a total photometric error in (2MASS and UltraVISTA, summed in quadrature) of less than 0.2 mag. The thick solid line shows a running median which is always within approximately 0.05 magnitudes of zero for  $15.0 < \text{mag} < 17.0$ . These curves are very similar to those plotted in McCracken et al. considering the uncertainties in the 2MASS photometry at these magnitudes.

In the right panel of Fig. 3 we compare the positions in right ascension and declination of point sources in 2MASS with those in our UltraVISTA  $K_s$  catalogue. As noted above, there is a small offset of  $0.1''$ .

#### 4.3.2 Limiting magnitudes and seeing

The  $5\sigma$  noise in the stacks in  $2''$  apertures was computed using empty apertures (regions of the images which contained no pixels identified as objects). Three different procedures were used which gave results that agreed to within 0.1 magnitudes.<sup>6</sup> The results from one of the procedures was chosen to be used for the headers. An approximate aperture correction (from  $2''$  to total magnitude) of 0.3 mag was subtracted (this was derived as the typical magnitude difference for point sources between  $2.0''$  and  $7.1''$  diameter aperture magnitudes). The resulting limiting magnitudes were written to the headers and are listed in Tab. 1. The noise computation was done separately for the ultra-deep and deep stripes.

Table 1 also lists the typical exposure times per pixel, in hours, for the two sets of stripes. These values are calculated as the total time spent on the given set of stripes, multiplied by  $2/3$ , reflecting that a typical point (pixel) on the sky will be covered by 2 of the 3 pawprints that make up a given set of stripes. If all the typical exposure times per pixel values in Tab. 1 (both for the ultra-deep and the deep stripes) are summed and multiplied by  $3/2$  one recovers the total exposure time in this release of 1287.5 hours mentioned in Sect. 2.

<sup>6</sup>When the difference between the noise in DR3 and DR4 was computed, the agreement between the procedures was better; for example, in the  $K_s$  band in the deep stripes, two of the procedures indicated the improvement in noise was 0.86 mag and 0.87 mag, respectively.

The PSF FWHM and ellipticity in the stacks (not split by stripes) was measured using `PSFex`, and are also listed in Tab. 1.

#### 4.4 Known issues

Users of DR4 should be aware of these two principal changes compared to previous releases, already described in this document:

- The change of the astrometric reference frame from 2MASS to Gaia, which introduces a shift of  $\sim 0.1''$  with respect to our previous releases.
- During the coaddition, the noisy SE region of chip 16 has no longer been masked. This means that the total area of the survey has increased slightly compared to previous releases. Users should carefully assess the photometric quality of the regions of the stacks which were masked in previous releases.

#### 4.5 Previous releases

The entire set of files in DR4 (stacks, sources lists and the 5-band catalogue) supersedes – or in the new Phase 3 language: *updates* – the corresponding data products from DR3 and previous releases.

The "DR2.1" release, which is the Laigle et al. (2016) multi-band (ca. 30 bands) catalogue based on the UltraVISTA DR2 images and other data (UV, optical, IR, ...), is not "superseded" (updated) by this DR4 release (a new public multi-band catalogue based on UltraVISTA DR4 is in preparation).

#### 4.6 Software versions

DR4 makes extensive use of the `astromatic` software. A complete list of software versions used is listed in Table 2.

| Software name              | Version |
|----------------------------|---------|
| <code>SExtractor</code>    | 2.24.2  |
| <code>PSFex</code>         | 3.18.2  |
| <code>Scamp</code>         | 2.6.3   |
| <code>SWarp</code>         | 2.38.0  |
| <code>WeightWatcher</code> | 1.12    |
| <code>MissFITS</code>      | 2.8.0   |

**Table 2:** Software versions used in UltraVISTA DR4.



## 5 Data format

### 5.1 File types

All images and catalogues are distributed in FITS format. In this release, we provide five stacked images and their corresponding weight maps for  $Y$ ,  $J$ ,  $H$ ,  $K_s$ , and NB118 narrow-band data composed of images from the first seven years of the UltraVISTA public survey.

Given the deep and ultra-deep sections have different exposure times, this has the important consequence that the signal-to-noise ratio for an object of a given magnitude will vary across the image. An inspection of the weight map provided with each image will indicate the location of the deeper zones.

Images have a zero-point of 30.0 AB magnitudes for a one second equivalent exposure time. The conversion Vega-to-AB follows the offsets given in McCracken et al. (2012). The images have a pixel scale of  $0.15''/\text{pixel}$  and have a common tangent point, in decimal RA, DEC (J2000) of (150.116, 2.2000). This is the tangent point of the publicly available IRSA/COSMOS images. Each image is  $\sim 9\text{GB}$  in size.

Following the ESO Phase 3 standard, the FITS files for the 5 stacks are multi-extension FITS files, with the stacked image in the primary HDU (header data unit) and with a “provenance table” in the first (and only) extension. The provenance table lists all the raw images that (after processing at CASU and CALET) were combined to make the given stack. The FITS files for the weight maps for the stacks have the same provenance tables as the FITS files for the stacks.

### 5.2 Complete list of distributed products

Tables 3 and 4 list the imaging, source list and catalogue data products distributed in DR4. Five images are provided, as well as their corresponding weight maps. These weight-maps correspond to the MAP\_WEIGHT images produced by SWarp and have pixel values proportional to the inverse variance. Note that the weight maps do not show up in the archive query<sup>7</sup>, but are added to the download when you request the corresponding images/stacks. We also note that we plan to put all the 20 DR4 files on our website<sup>8</sup>.

We provide several source list products: “dual-mode” ones, in which the  $K_s$  image is used as the detection image and each of the other images in turn is used as the measurement image; and “single band” images in which each individual image is used in turn as both measurement and detection image. Dual-mode source lists have the advantage that, as the same number of entries is present in all source lists, colours can be easily computed for each object. The second source list type contains, in principle, all sources to a given detection threshold ( $1.8\sigma$ ). Source lists were extracted using SExtractor (Bertin & Arnouts 1996) version 2.24.2 compiled and downloaded from the astromatic.net<sup>9</sup>. For each entry in the source list we provide flux measurements in 18 photometric apertures. Their diameters in pixels ( $1\text{ px} = 0.15''$ ) are as follows, corresponding to three apertures of  $2''$ ,  $3''$  and  $7.1''$  and logarithmically spaced apertures from  $0.5''$  to  $5''$ :

---

<sup>7</sup>[http://archive.eso.org/wdb/wdb/adp/phase3\\_main/form?collection\\_name=UltraVISTA&release\\_name=DR4](http://archive.eso.org/wdb/wdb/adp/phase3_main/form?collection_name=UltraVISTA&release_name=DR4)

<sup>8</sup><http://www.ultravista.org/>

<sup>9</sup><http://astromatic.net/software/sextractor>

13.33, 20.00, 47.33, 3.33, 3.93, 4.63, 5.46, 6.44, 7.59, 8.94,  
 10.54, 12.43, 14.65, 17.26, 20.35, 23.99, 28.28, 33.33

We also provide a merged 5-band catalogue `UVISTA_5band_cat_dr4_rc_v2.fits` created from the individual  $K_s$ -selected source lists. The columns in this catalogue are described in Table 5. Two additional columns are provided: the  $E(B - V)$  Galactic reddening value measured at the position of each galaxy in the Schlegel et al. (1998) dust maps, together with a flag which indicates the field border.

| Filename   | Description       |
|--|-------------------|
| <code>UVISTA_Y_19_11_18_allpaw_skysub_015_dr4_rc_v2.fits</code>            | Y-band stack      |
| <code>UVISTA_Y_19_11_18_allpaw_skysub_015_dr4_rc_v2.weight.fits</code>     | Y-band weight     |
| <code>UVISTA_J_19_11_18_allpaw_skysub_015_dr4_rc_v2.fits</code>            | J-band stack      |
| <code>UVISTA_J_19_11_18_allpaw_skysub_015_dr4_rc_v2.weight.fits</code>     | J-band weight     |
| <code>UVISTA_H_19_11_18_allpaw_skysub_015_dr4_rc_v2.fits</code>            | H-band stack      |
| <code>UVISTA_H_19_11_18_allpaw_skysub_015_dr4_rc_v2.weight.fits</code>     | H-band weight     |
| <code>UVISTA_Ks_19_11_18_allpaw_skysub_015_dr4_rc_v2.fits</code>           | Ks-band stack     |
| <code>UVISTA_Ks_19_11_18_allpaw_skysub_015_dr4_rc_v2.weight.fits</code>    | Ks-band weight    |
| <code>UVISTA_NB118_19_11_18_allpaw_skysub_015_dr4_rc_v2.fits</code>        | NB118-band stack  |
| <code>UVISTA_NB118_19_11_18_allpaw_skysub_015_dr4_rc_v2.weight.fits</code> | NB118-band weight |

**Table 3:** Summary of DR4 stacked images and weight maps. All images have a zero point of 30.0 AB magnitudes for a one second equivalent exposure time and a scale of  $0.15''/\text{pixel}$ .

| Filename   | Detection | Measurement          |
|--|-----------|----------------------|
| <code>UVISTA_Ks_19_11_18_allpaw_skysub_015_dr4_rc_v2.cat.fits</code>       | $K_s$     | $K_s$                |
| <code>UVISTA_Ks_19_11_18_allpaw_skysub_015_dr4_rc_v2_Y.cat.fits</code>     | $K_s$     | $Y$                  |
| <code>UVISTA_Ks_19_11_18_allpaw_skysub_015_dr4_rc_v2_J.cat.fits</code>     | $K_s$     | $J$                  |
| <code>UVISTA_Ks_19_11_18_allpaw_skysub_015_dr4_rc_v2_H.cat.fits</code>     | $K_s$     | $H$                  |
| <code>UVISTA_Ks_19_11_18_allpaw_skysub_015_dr4_rc_v2_NB118.cat.fits</code> | $K_s$     | NB118                |
| <code>UVISTA_Y_19_11_18_allpaw_skysub_015_dr4_rc_v2.cat.fits</code>        | $Y$       | $Y$                  |
| <code>UVISTA_J_19_11_18_allpaw_skysub_015_dr4_rc_v2.cat.fits</code>        | $J$       | $J$                  |
| <code>UVISTA_H_19_11_18_allpaw_skysub_015_dr4_rc_v2.cat.fits</code>        | $H$       | $H$                  |
| <code>UVISTA_NB118_19_11_18_allpaw_skysub_015_dr4_rc_v2.cat.fits</code>    | NB118     | NB118                |
| <code>UVISTA_5band_cat_dr4_rc_v2.fits</code>                               | $K_s$     | $YJHK_s\text{NB118}$ |

**Table 4:** Source list and catalogue products delivered with DR4.

| Column number | Column name        | Description  |
|---------------|--------------------|--|
| 1             | SOURCE_ID*         | UltraVISTA source designation (DR4)                                |
| 2             | NUMBER*            | Running object number  |
| 3             | ALPHA_J2000*       | Right ascension of barycenter in decimal degrees (J2000)           |
| 4             | DELTA_J2000*       | Declination of barycenter in decimal degrees (J2000)               |
| 5             | X_IMAGE*           | Object position along x  |
| 6             | Y_IMAGE*           | Object position along y  |
| 7             | FLAG_HJMCC*        | Bad region flag: != 0 for bad region (field boundaries: 1)         |
| 8             | EBV*               | Galactic reddening E(B-V) based on Schlegel et al (1998) dust maps |
| 9             | Y_APER2*           | Y fixed aperture magnitude (2")                                    |
| 10            | Y_APER2_ERR*       | Y fixed aperture mag error (2")                                    |
| 11            | Y_APER7*           | Y fixed aperture magnitude (7.1")                                  |
| 12            | Y_APER7_ERR*       | Y fixed aperture mag error (7.1")                                  |
| 13            | Y_AUTO*            | Y auto magnitude   |
| 14            | Y_AUTO_ERR*        | Y auto mag error   |
| 15            | Y_FLUX_RADIUS*     | Radius of aperture containing half the flux of Y_MAG_AUTO          |
| 16            | Y_FLAG*            | Y Flag (sextractor)  |
| 17            | J_APER2*           | J fixed aperture magnitude (2")                                    |
| 18            | J_APER2_ERR*       | J fixed aperture mag error (2")                                    |
| 19            | J_APER7*           | J fixed aperture magnitude (7.1")                                  |
| 20            | J_APER7_ERR*       | J fixed aperture mag error (7.1")                                  |
| 21            | J_AUTO*            | J auto magnitude   |
| 22            | J_AUTO_ERR*        | J auto mag error   |
| 23            | J_FLUX_RADIUS*     | Radius of aperture containing half the flux of J_MAG_AUTO          |
| 24            | J_FLAG*            | J Flag (sextractor)  |
| 25            | H_APER2*           | H fixed aperture magnitude (2")                                    |
| 26            | H_APER2_ERR*       | H fixed aperture mag error (2")                                    |
| 27            | H_APER7*           | H fixed aperture magnitude (7.1")                                  |
| 28            | H_APER7_ERR*       | H fixed aperture mag error (7.1")                                  |
| 29            | H_AUTO*            | H auto magnitude   |
| 30            | H_AUTO_ERR*        | H auto mag error   |
| 31            | H_FLUX_RADIUS*     | Radius of aperture containing half the flux of H_MAG_AUTO          |
| 32            | H_FLAG*            | H Flag (sextractor)  |
| 33            | KS_APER2*          | Ks fixed aperture magnitude (2") [detection image]                 |
| 34            | KS_APER2_ERR*      | Ks fixed aperture mag error (2") [detection image]                 |
| 35            | KS_APER7*          | Ks fixed aperture magnitude (7.1") [detection image]               |
| 36            | KS_APER7_ERR*      | Ks fixed aperture mag error (7.1") [detection image]               |
| 37            | KS_AUTO*           | Ks auto magnitude [detection image]                                |
| 38            | KS_AUTO_ERR*       | Ks auto mag error [detection image]                                |
| 39            | KS_FLUX_RADIUS*    | Radius of aperture containing half the flux of KS_MAG_AUTO         |
| 40            | KS_FLAG*           | Ks Flag (sextractor) [detection image]                             |
| 41            | NB118_APER2*       | NB118 fixed aperture magnitude                                     |
| 42            | NB118_APER2_ERR*   | NB118 fixed aperture mag error                                     |
| 43            | NB118_APER7*       | NB118 fixed aperture magnitude                                     |
| 44            | NB118_APER7_ERR*   | NB118 fixed aperture mag error                                     |
| 45            | NB118_AUTO*        | NB118 auto magnitude   |
| 46            | NB118_AUTO_ERR*    | NB118 auto mag error   |
| 47            | NB118_FLUX_RADIUS* | Radius of aperture containing half the flux of NB118_MAG_AUTO      |
| 48            | NB118_FLAG*        | NB118 Flag (sextractor)  |

**Table 5:** Complete list of columns in the five-band merged catalogue. All magnitudes are in the AB system. A star (\*) after the column name indicates that the TINDX*i* header keyword set to T, which in turn is related to how the ESO catalogue facility indexes the data.

## 6 Release of the CASU single OB pawprint stacks at VSA/WFAU

As part of the VISTA Data Flow System (e.g. Emerson et al. 2004), CASU produces stacks of the data contained in a single OB and on a single pawprint (e.g. Irwin et al. 2004; Lewis et al. 2010, and the CASU web site<sup>10</sup>). These stacks have `_st` in the file names and are sometimes called `_st` stacks. The UltraVISTA OBs typically comprise 0.5 or 1 hour exposure on a given pawprint, and in UltraVISTA we have somewhat imprecisely referred to these CASU stacks as the “1-hour stacks”. Throughout the UltraVISTA program we have supplied these stacks to interested parties on a best-effort basis and these data (from seasons 1–5) have recently been exploited in a new AGN variability study (Sánchez et al. 2017). However, to make these data more widely available we are releasing these stacks through the VISTA Science Archive (VSA, e.g. Hambly et al. 2004; Cross et al. 2012) at the Wide Field Astronomy Unit (WFAU) at Edinburgh, concurrent with the ESO data release of our deep stacks.

It should be noted that our deep stacks are made by redoing the sky subtraction of the individual images corresponding to 1 or 2 minutes of exposure and then stacking these; our deep stacks are not made by stacking the CASU `_st` stacks. We have not used the CASU stacks in our processing, and we are providing them via the VSA “as is”. The VSA was already serving data from 5 of the 6 original VISTA surveys (VHS, VVV, VMC, VIKING and VIDEO).

The VSA will not only allow the user to download selected or all of the CASU stacks and their confidence maps, it will also allow the user to upload a text file with coordinates of one or more objects, and then in a second step get the photometry from each CASU stack, giving a table including aperture-corrected magnitude and time (MJD OBS), from which a light curve in the five UltraVISTA bands can be plotted.

### 6.1 The CASU single OB pawprint stacks at the VSA

#### 6.1.1 Cookbook: How to download the CASU single OB pawprint stacks and their confidence maps

Go to the VSA (VISTA Science Archive) home page <http://surveys.roe.ac.uk/vsa>

There is no need to login

Click “Archive Listing”

Under “Select the programme/survey you wish to use:” select “UltraVISTA”

Under “Database release to use:” select “ULTRAVISTADR4”

Under “Observation type:” leave it at “object”

Under “Frame type:” select “stack (pawprint)”

Possibly limit by filter or time period

Possibly increase “Rows per page:” up to a max of 1000

Click GetList

Then download the CASU single OB pawprint stacks via the “Link to image wget script” link

To get the CASU confidence maps for these stacks, in the form do:

Under “Observation type:” select “confidence”

Under “Frame type:” select “stack (pawprint)” (as before)

---

<sup>10</sup><http://casu.ast.cam.ac.uk/surveys-projects/vista/technical/data-processing>

### 6.1.2 Number of CASU single OB pawprint stacks vs number of OBs

We mentioned in Sect. 2 that we had downloaded 63,931 individual images (images typically corresponding to 1 or 2 minutes of exposure) from CASU. The number of unique values of the `HIERARCH ESO OBS ID` header keyword, i.e. the number of OBs, is 1719. As also mentioned, after our quality control cuts we were left with 58,138 individual images which were used to make our 5 stacks; these correspond to 1716 OBs. Then to the VSA: the first query in the above cookbook will return 2108 CASU single OB pawprint stacks, from the one with

```
multiframeID = 1588267
dateObs = 2009-12-05 07:07:56.1
obsName = ultravista-Y-paw1-001
```

to the one with

```
multiframeID = 4101807
dateObs = 2016-06-29 23:13:00.6
obsName = ultravista11-K-shortOB-paw1-CS2-011
```

where `multiframeID` is a unique ID added by the VSA. If you make a unique list of the OB names listed on the VSA under `obsName`, you get 1726 OBs. We had expected that to be the 1719 OBs mentioned above. The VSA list contains 7 unique OB names not found in the data we downloaded from CASU ourselves; these 7 OBs each appear once in the VSA list with these values of `dateObs` and `obsName`:

```
2013-04-27 23:36:27.9 ultravista9-H-shortOB-paw3-CS2-003
2013-04-28 00:19:56.0 ultravista9-H-shortOB-paw1-CS2-004
2013-04-28 01:01:06.0 ultravista9-H-shortOB-paw2-CS2-004
2013-04-28 01:42:20.1 ultravista8-J-paw3-CS2-002
2013-04-28 02:55:44.7 ultravista9-J-shortOB-paw3-CS2-001
2016-05-19 23:52:33.8 ultravista15-K-shortOB-paw1-CS3-003
2016-05-20 01:22:37.4 ultravista15-K-shortOB-paw2-CS3-003
```

It seems that somehow when we downloaded data from CASU to make the UltraVISTA stacks, we did not get the data for the nights starting 20130427 and 20160519.

That detail aside, the reason that the number of CASU single OB pawprint stacks at the VSA is 2108 when the number of OBs at the VSA only is 1726 is mainly that a given OB can be observed more than once: if the quality control carried out at Paranal deems the OB needs to be repeated (typically if the seeing constraint was violated by more than 10%), the OB will be repeated, resulting in two (or more) stacks for the same OB. Additionally, a few of our OBs (namely some of the NB118 OBs from the first season) do 3 pawprints in a single OB, and thus result in 3 stacks.

### 6.1.3 The deprecation code used at the VSA

The above-mentioned query at the VSA returns 2108 CASU single OB pawprint stacks. In terms of the column called `deprecated`, 624 stacks are listed with a value of 18 (hereafter deprecated

stacks) and 1484 stacks are listed with a value of 0. The definition is based on the list of individual images (“normal images” in the WFAU terminology) used to make the given CASU single OB pawprint stack (typically 15, 30 or 60 images), and the list of 58,138 individual images used to make the UltraVISTA stacks (“deep stacks”). Specifically, if less than 90% of the images used to make a given CASU single OB pawprint stack were used to make the UltraVISTA deep stack, then that CASU single OB pawprint stack is defined as deprecated. That level of 90% is somewhat arbitrary, but intended as a reasonable way of quickly flagging up suspect OB stacks. These stacks probably just have a slightly worse seeing than average, and the user is advised to check all stacks.

## 7 Acknowledgements

This UltraVISTA release has been made possible thanks to a significant infrastructure grant from “Domaine d’intérêt majeur en astrophysique et conditions d’apparition de la vie (DIM-ACAV+)”. HJMCC acknowledges financial support from the “Programme national cosmologie et galaxies” (PNCG). This research has made use of the VizieR catalogue access tool provided by the CDS, Strasbourg, France. JPUF and BMJ acknowledge support from the ERC-StG grant EGG-278202. The Cosmic Dawn Center is funded by the Danish National Research Foundation. OLF acknowledges support from the ERC advanced grant ERC-2010-AdG-268107. JSD acknowledges the support of the Royal Society via a Wolfson Research Merit award, and also the support of the European Research Council via the award of an Advanced Grant. The UltraVISTA team would like to thank ESO staff for scheduling and making the UltraVISTA observations, and the Cambridge Astronomy Survey Unit for providing us with pre-processed UltraVISTA images. We thank E. Bertin for many useful discussions concerning the usage of the `Astromatic` tool set.

## References

- Bertin, E. & Arnouts, S. 1996, *ApJS*, 117, 393
- Cross, N. J. G., Collins, R. S., Mann, R. G., et al. 2012, *A&A*, 548, A119
- Emerson, J. P., Irwin, M. J., Lewis, J., et al. 2004, in *Society of Photo-Optical Instrumentation Engineers (SPIE) Conference Series*, Vol. 5493, *Society of Photo-Optical Instrumentation Engineers (SPIE) Conference Series*, ed. P. J. Quinn & A. Bridger, 401–410
- Gaia Collaboration, Brown, A. G. A., Vallenari, A., et al. 2016, *Astronomy & Astrophysics*, 595, A2
- Gruen, D., Seitz, S., & Bernstein, G. M. 2014, *Publications of the Astronomical Society of the Pacific*, 126, 158
- Hambly, N. C., Mann, R. G., Bond, I., et al. 2004, in *Society of Photo-Optical Instrumentation Engineers (SPIE) Conference Series*, Vol. 5493, *Society of Photo-Optical Instrumentation Engineers (SPIE) Conference Series*, ed. P. J. Quinn & A. Bridger, 423–431

- Irwin, M. J., Lewis, J., Hodgkin, S., et al. 2004, in Society of Photo-Optical Instrumentation Engineers (SPIE) Conference Series, Vol. 5493, Society of Photo-Optical Instrumentation Engineers (SPIE) Conference Series, ed. P. J. Quinn & A. Bridger, 411–422
- Laigle, C., McCracken, H. J., Ilbert, O., et al. 2016, *ApJS*, 224, 24
- Lewis, J. R., Irwin, M., & Bunclark, P. 2010, in Astronomical Society of the Pacific Conference Series, Vol. 434, Astronomical Data Analysis Software and Systems XIX, ed. Y. Mizumoto, K.-I. Morita, & M. Ohishi, 91
- McCracken, H. J., Milvang-Jensen, B., Dunlop, J., et al. 2012, *A&A*, 544, A156
- Sánchez, P., Lira, P., Cartier, R., et al. 2017, *ApJ*, 849, 110
- Schlegel, D. J., Finkbeiner, D. P., & Davis, M. 1998, *ApJ*, 500, 525
- Scoville, N., Aussel, H., Brusa, M., et al. 2007, *ApJS*, 172, 1
- Skrutskie, M. F., Cutri, R. M., Stiening, R., et al. 2006, *AJ*, 131, 1163